HHS Public Access

Author manuscript

Nucl Med Biol. Author manuscript; available in PMC 2016 January 01.

Published in final edited form as:

Nucl Med Biol. 2015 January ; 42(1): 46–52. doi:10.1016/j.nucmedbio.2014.08.010.

In Vivo Detection of Hyperoxia-Induced Pulmonary Endothelial Cell Death Using ^{99m}Tc-Duramycin

Said H. Audi[1,2], **Elizabeth R. Jacobs**[2,3], **Ming Zhao**[4], **David L. Roerig**[3,5,6], **Steven T. Haworth**[2], and **Anne V. Clough**[1,2,7]

[1]Department of Biomedical Engineering, Marquette University

[2]Division of Pulmonary and Critical Care Medicine, Medical College of Wisconsin

[3]Zablocki V.A. Medical Center

[4]Division of Cardiology, Feinberg School of Medicine, Northwestern University

[5]Department of Anesthesiology, Medical College of Wisconsin

[6]Department of Pharmacology/Toxicology, Medical College of Wisconsin

[7]Department of Mathematics, Statistics, and Computer Science, Marquette University

Abstract

Introduction: ^{99m}Tc-duramycin, DU, is a SPECT biomarker of tissue injury identifying cell death. The objective of this study is to investigate the potential of DU imaging to quantify capillary endothelial cell death in rat lung injury resulting from hyperoxia exposure as a model of acute lung injury.

Methods: Rats were exposed to room air (normoxic) or >98% O_2 for 48 or 60 hours. DU was injected i.v. in anesthetized rats, scintigraphy images were acquired at steady-state, and lung DU uptake was quantified from the images. Post-mortem, the lungs were removed for histological studies. Sequential lung sections were immunostained for caspase activation and endothelial and epithelial cells.

Results: Lung DU uptake increased significantly ($p < 0.001$) by 39% and 146% in 48-hr and 60-hr exposed rats, respectively, compared to normoxic rats. There was strong correlation ($r^2 = 0.82$, $p = 0.005$) between lung DU uptake and the number of cleaved caspase 3 (CC3) positive cells, and endothelial cells accounted for more than 50% of CC3 positive cells in the hyperoxic lungs. Histology revealed preserved lung morphology through 48 hours. By 60 hours there was evidence of edema, and modest neutrophilic infiltrate.

Corresponding Author: Anne V. Clough, Ph.D., Department of Mathematics, Statistics and Computer Science, Marquette University, PO Box 1881, Milwaukee, WI 53201-1881, Phone: 414-288-5238, Fax: 414-384-0115, anne.clough@marquette.edu.

CONFLICT OF INTEREST

Nothing to disclose.

Conclusions: Rat lung DU uptake in vivo increased after just 48 hours of >98% O_2 exposure, prior to the onset of any substantial evidence of lung injury. These results suggest that apoptotic endothelial cells are the primary contributors to the enhanced DU lung uptake, and support the utility of DU imaging for detecting early endothelial cell death in vivo.

Keywords

Apoptosis; lung imaging; acute lung injury

INTRODUCTION

Acute lung injury (ALI) is characterized by rapidly progressing hypoxic lung failure following a direct or indirect injury to the pulmonary parenchyma or vasculature [1]. This condition is one of the most frequent causes of admission to medical intensive care units, and of the approximately one million patients receiving invasive mechanical ventilation per year, 10% develop new ALI [2]. The most serious form of ALI is Acute Respiratory Distress Syndrome (ARDS) which occurs in ~200,000 patients in the U.S. per year and carries a mortality rate of nearly 40% despite the best supportive care [3].

Recent studies suggest that ~70% of ALI patients are not recognized as such by bedside providers, and stress the importance of early detection of ALI (i.e. prior to clinical evidence) for enhancing the efficacy of existing therapies and improving outcomes of ALI/ARDS patients [3,4]. Beyond antibiotics, patients at risk for ALI development would be strong candidates for strategies including limited blood transfusions (to avoid transfusion related lung injury), closer clinical observation (such as in an intermediate care unit), limitation of inhaled oxygen fractions to levels needed to support vital organ function, but not more, and strict attention to intake and output measurements to detect fluid retention and pulmonary edema. Each of these interventions is not universally implemented because of risk to benefit ratios. Thus, our long-term goal is to develop a clinical means for early detection and monitoring of ALI in individual patients.

Rat exposure to lethal (>95%) concentrations of oxygen (hyperoxia) is a well-documented model of human ALI/ARDS [5-8]. Crapo et al. [7] provide a detailed description of histologic and morphometric changes in lungs of rats exposed to 100% O_2. No structural changes are observed in lungs of rats exposed to 100% O_2 for up to 40 hours. However, by 60 hours, there is a 30% loss in capillary endothelial cells due to cell death, infiltration of phagocytic cells, thickening of the air-blood barrier, and pleural effusion. This is followed by further loss in endothelial cells and edema, pleural effusion, severe hypoxemia, and death within 72 hours [7]. There is strong evidence that the pulmonary capillary endothelium is a primary and early site of oxygen toxicity injury [7,9,10]. This and the large pulmonary capillary surface area in direct apposition with blood-borne compounds suggest the utility of biomarker imaging for detecting early lung endothelial injury due to hyperoxic ALI [11,12].

^{99m}Tc-duramycin, DU, is a new SPECT biomarker sensing cell death via apoptosis and/or necrosis [12-14]. DU serves as a molecular probe that binds to phosphatidylethanolamine (PE), which has little presence on the surface of normal viable cells, but becomes exposed onto the cell surface and/or accessible to the extracellular milieu with apoptosis and

necrosis, respectively [13,14]. Recently we reported an increase in the lung uptake of DU in rats exposed to sublethal 85% O_2 [12]. The objective of the present study is to determine the extent of DU lung uptake in rats injured with >98% O_2 exposure for up to 60 hours, and to correlate that uptake with capillary endothelial cell apoptosis detected histologically.

MATERIALS AND METHODS

Duramycin (3,035 g/mole MW) kits were prepared as previously described [12], and technetium-labeled macroaggregated albumin (^{99m}Tc-MAA, particle sizes 20 – 40 μm) was purchased from Cardinal Health (Wauwatosa, WI). Antibodies to cleaved caspase 3 (Biocare, #CP229B), CD31 (Acris, #AP15436PU-N), keratin 7 (Abcam, #9021), and myeloperoxidase (Abcam, #45977) were used with appropriate secondary antibodies (Jackson Immuno #711-066-152 for CD31, Jackson Immuno #715-066-151 for keratin 7, and Abcam #6829 HRP for MPO) to identify endpoints of interest. Other reagent grade chemicals were purchased from Sigma Chemical Company.

Animals

For normoxic (control) lung studies, adult (68-77 days old) male Sprague-Dawley rats (Charles River; 300-375 g) were exposed to room air. For hyperoxic lung studies, rats within the same weight and age range of normoxic rats were housed in a Plexiglass chamber maintained at >98% O_2 for either 48 or 60 hrs as previously described [11]. A total of fifteen normoxic, twelve 48-hr, and seventeen 60-hr rats were studied. The protocol was approved by the Institutional Animal Care and Use Committees of the Zablocki Veterans Affairs Medical Center and Marquette University (Milwaukee, WI). Rat imaging studies described below were conducted immediately following the hyperoxic exposure period.

Imaging Studies

Ten normoxic, seven 48-hr hyperoxic, and seven 60-hr hyperoxic rats were imaged using DU. These sample sizes achieve a power > 85% for detecting changes in lung uptake of DU greater than 15% based on previously published results with DU [12] (ANOVA power; SigmaPlot version 12.0).

Each rat was anesthetized with pentobarbital sodium (40-50 mg/kg, i.p.), and the left femoral vein cannulated (PE-10 tubing). The rat was then placed supine on a 4-mm thick plexiglass plate positioned directly on the face of a parallel-hole collimator attached to a modular gamma camera (Radiation Sensors, LLC) for planar imaging. An injection of ^{99m}Tc-duramycin (37-74 MBq) was prepared according to kit directions and administered i.v. Planar images were acquired every 1 second during the first minute and every 1 minute thereafter for 20 minutes. Approximately five minutes later without relocation of the rat, an injection of ^{99m}Tc-MAA (18-37 MBq) was made via the same cannula and the rat re-imaged at 1 frame/min for 5 minutes. The ^{99m}Tc-MAA injection provided planar images in which the lung boundaries were clearly identified, since >95% of ^{99m}Tc-MAA lodged in the lung. After imaging, the rats were euthanized with an overdose of pentobarbital sodium. For a subset of these normoxic and hyperoxic rats, the lungs were removed, fixed inflated with paraformaldehyde to allow for ^{99m}Tc decay, and then used for histological studies.

DU Image Analysis

The boundaries of the upper portion of the lungs identified in the high-sensitivity ^{99m}Tc-MAA images were manually outlined to construct a lung region of interest (ROI) free of any liver contribution [12]. The ^{99m}Tc-MAA generated lung ROI mask was then superimposed on the time sequence of DU images yielding a lung DU ROI as shown in Figure 1. Background regions in the upper forelimbs were identified in the DU images to normalize lung activity for injected biomarker specific activity, dose, and decay [12]. Time-activity curves depicting mean counts/min/pixel within the lung and forelimb-background ROIs were then acquired. The ratio of the lung and background ROI signals averaged over the last 3 minute time interval of the 20-minute acquisition period, was used as the measure of lung steady-state DU uptake [11,12].

Histological Studies

Lungs from six normoxic, six 48-hr hyperoxic, and five 60-hr hyperoxic rats were paraffin-embedded, sectioned in 4 μm thick whole mounts, and then stained with hematoxylin and eosin (H&E).

Lung sections from four of the normoxic lungs and all of the hyperoxic lungs were immunostained with antibody to cleaved caspase 3 (CC3, a marker of caspase activation). For four lungs from each of the three groups, sequential lung sections were also immunostained for either CD31, to identify endothelial cells, or keratin 7, to identify epithelial cells. Sections could not be co-stained with antibodies to both CC3 and keratin 7 or CD31 because all positive cells appear brown. Image analysis was performed on jpeg images of whole mounts. To quantify apoptosis, we divided the whole mount sections into six sections, then blindly identified an ROI roughly 1mm by 1mm, devoid of large airways or vessels from each section and acquired an image at a fixed 10X magnification of CC3-stained sections. The numbers of CC3 positive cells per each image were counted by one observer blinded to the treatment groups.

In a separate analysis with the observer blinded to the treatment group, cells in images which clearly exhibited CC3 staining were matched with either CD31 or keratin 7 in sequential sections to quantify apoptotic endothelial or epithelial cells.

Additional lung sections from five normoxic, four 48-hr hyperoxic, and four 60-hr hyperoxic rats were immunostained for myeloperoxidase (MPO) as a marker of neutrophil recruitment using a primary antibody to MPO with matched isotype HRP-conjugated secondary antibody. MPO density in two to six representative images of lung sections per rat was quantified by an observer blinded to the treatment group using MetaMorph in a manner previously reported by us [15]

Lung Wet-To-Dry Weight Ratio, Weight of Pleural Effusion

For a subset of the normoxic and hyperoxic rats, pleural effusion and lung wet-to-dry weight ratios were measured as previously described [13,16]. Briefly, the chest cavity was opened and cotton gauze was inserted into the chest cavity to absorb any pleural effusion. The difference in the weight of the gauze pre- and post-insertion yielded the pleural effusion

weight. The lungs were then removed, weighed, and then dried (60 °C) to a constant weight to obtain the lung wet-to-dry weight ratio.

Statistical evaluation of data was carried out using SigmaPlot version 12.0 (Systat Software Inc., San Jose, CA). Intraclass correlations were calculated using publicly accessible SAS macros (%magree and %intracc). The level of statistical significance was set at $p < 0.05$. Values are mean ± SEM unless otherwise indicated.

RESULTS

Rats did not display any sign of distress after 48 hrs of hyperoxic exposure. However by 60 hrs, rats exhibited decreased intake of food and water and some demonstrated respiratory distress, especially upon removal from the chamber. Pleural effusion weight, which was negligible at 0 and 48 hours of hyperoxic exposure, measured 7.6 ± 1.6 g ($p < 0.001$) at 60 hrs (Table 1).

Body weight was measured as an index of general health status. Rats lost 6 ± 2 g (paired *t*-test, $p = 0.003$) and 18 ± 2 g ($p < 0.001$) of their pre-exposure body weight after 48 and 60 hrs of hyperoxic exposure, respectively.

For 48-hr hyperoxic rats, the wet-to-dry weight ratio increased by 15% ($p = 0.018$), although there was no significant change in lung wet weight or dry weight as compared to those of normoxic rats (Table 1). For 60-hr hyperoxic rats, lung wet weight increased by 66% ($p < 0.001$) and dry weight by 38% ($p < 0.001$), compared to normoxics (Table 1). As a result, the wet-to-dry weight ratio increased by only 20% ($p = 0.003$) and was not different from that of 48-hr hyperoxic rats (Table 1).

Figure 2A-C depicts representative H&E stained lung images of normoxic, 48-hr hyperoxic, and 60-hr hyperoxic rats. Images from normoxic rats show the lacey architecture of normal lungs with very thin alveolar capillary membranes to facilitate gas exchange. The 48-hr hyperoxic images were not obviously different from normoxic. In contrast, the 60-hr hyperoxic images exhibit perivascular edema, most evident in the low-power views. The alveolar capillary membrane appears thickened, seen best in the high-power views. Inflammatory cells within the perivascular spaces and the capillary interstitium can also be seen.

Since H&E staining did not readily distinguish details of inflammatory cell infiltrates, we also stained lung sections for myloperoxidase (MPO). Figure 2D-F shows an increase in the number of MPO positive cells (brown color) in the 60-hr sections relative to the 48-hr or normoxic slices. The average MPO thresholded area increased by 81% ($p = 0.02$) in 60-hr lung slices compared to normoxic slices (Table 2).

Typical in vivo DU lung images at steady-state from normoxic, 48-hr hyperoxic, and 60-hr hyperoxic rats are shown in Figure 3. Figure 4A shows representative lung and background DU time-activity curves obtained from the time sequence of images from the normoxic rat in Figure 3. Figure 4B shows the average lung and background DU time-activity curves and the corresponding lung-to-background ratio over the 1 – 20 min post-injection time period

obtained from the ten normoxic rats imaged. Lung and background activity and their ratio reached steady-state by ~20 min following DU injection.

Figure 5 shows the average DU lung-to-background ratios over the 1 – 20 min time period for all of the normoxic, 48-hr hyperoxic, and 60-hr hyperoxic rats imaged. For all three groups, the ratio reached steady-state by 20 min following DU injection. DU lung uptake, as measured by the lung-to-background DU ratio at steady-state, was increased (39%, $p < 0.001$) following 48 hrs of hyperoxia exposure and even further (146%, $p < 0.001$) at 60 hrs of exposure compared to normoxic rats (Figure 6). The reliability of the DU image analysis was evaluated by having a single operator blinded to the treatment group obtain three repeated measurements from all rats, resulting in an Intraclass Correlation Coefficient (ICC) of 0.98.

Lung slices immunostained with an antibody to CC3 showed that the number of CC3 positive cells per high-power field increased more than 2.5-fold ($p = 0.002$) in lungs from 60-hr hyperoxic rats as compared to normoxics. The ICC for a single observer blinded to the treatment group performing three repeated measurements on 30 images was 0.96. Inter-observer reliability of 3 investigators under the same conditions resulted in ICC of 0.75.

Figure 7 shows strong correlation (coefficient of determination = 0.82, $p = 0.005$) between DU lung uptake and the number of CC3 positive cells in slices obtained from the corresponding lungs.

Figure 8 shows representative sequential lung slices immunostained with antibodies to CC3 and with either CD31 (endothelial cells) or keratin 7 (epithelial cells) from lungs of 60-hr hyperoxic rats. Overall, of the CC3 positive cells 53 ± 4% were CD31 positive and 17 ± 4% were keratin 7 positive. For normoxic lung slices, 27 ± 6% of CC3 positive cells were CD31 positive and 44 ± 8% were keratin 7 positive. For 48-hr hyperoxic lungs, 59 ± 4% were CD31 positive and 22 ± 4% were keratin 7 positive (Table 2). Unknown cells accounted for 30 ± 8%, 19 ± 6%, and 29 ± 7 % of total CC3 positive cells in lung slices from normoxic, 48-hr hyperoxic, and 60-hr hyperoxic rats, respectively (Table 2).

DISCUSSION

We report an increase in lung DU uptake measured in vivo after just 48 hours of >98% O_2 exposure, prior to the onset of significant histologic or functional evidence of lung injury. Moreover, we identified a strong correlation between DU lung uptake and the number of CC3 positive cells. Since more than 50% of CC3 positive cells were endothelial cells, apoptotic endothelial cells appear to contribute more to the enhanced DU lung uptake signal in hyperoxic rats than other cell types.

In this study we used in vivo planar imaging with a single modular gamma camera. Planar imaging greatly reduces the total scan time, requires no reconstruction, and with the methods described in the present study, image analysis is straightforward. Hyperoxic lung injury is thought to be a relatively homogeneous injury throughout the lung so that the 3D benefit of SPECT would not be expected to provide substantive additional information about DU uptake within the lung.

Several studies have demonstrated hyperoxia-induced apoptosis in the rat lung [17-20]. Otterbein et al. showed no increase in the number of TUNEL-positive cells (as a marker of apoptosis) in lung slices of rats exposed to 100% O_2 for 48 hours, but a sharp increase (~60-fold) after 61 hrs of exposure [19]. Kawamura et al. demonstrated a ~16-fold increase in the number of CC3 positive cells in lung sections of rats exposed to 100% O_2 for 60 hrs [17]. Howlett et al. reported that the number of TUNEL-positive cells (as a % of total cells) in lung sections increased from <1% in normoxic to 12% in 60-hr hyperoxic rats [18]. Sun et al. showed that the number of TUNEL-positive cells increased from ~5% in normoxic rat lungs to ~30% in 60-hr hyperoxic lungs [20]. In the present study, we report ~2.5-fold increase in the number of CC3 positive cells in 60-hr hyperoxic lungs (Table 2).

Our IHC results demonstrate that endothelial cell death accounts for more than 50% of apoptotic lung cells in hyperoxic lungs, and by implication, that pulmonary endothelial cell death dominates the enhanced DU lung uptake signal in hyperoxic rats (Figure 6). Hyperoxia-induced endothelial cell death was also reported in a study by Crapo et al. which showed that rat exposure to 100% O_2 for 60 hours resulted in a 30% loss in the number of pulmonary endothelial cells [7].

In the present study, a cell that stains for CD31 or keratin 7 is considered to be an apoptotic endothelial or epithelial cell, respectively, if it co-localizes with a cleaved caspase 3 positive cell in an adjacent slide (Figure 8). One limitation of this approach is that the percentage of identified cells for normoxic and hyperoxic lungs likely represents a lower threshold for matching of CC3 positive and markers for endothelial or epithelial cells because CD31 or keratin 7 protein may be missed in thin sections in some cells that have one or the other. This limitation is mitigated by the fact that the slide thickness (4 μm) is small relative to the diameter of an endothelial or epithelial cell (10-20 μm). As such, identified apoptotic endothelial and epithelial cells accounted for 70-80% of total number of apoptotic cells (CC3 positive) in lung slides from all three groups of rats (Table 2).

For lungs of 48-hr hyperoxic rats, no cellular infiltration was detected by either the lung dry weights or histology, suggesting little contribution of cellular infiltrate cell death to the increase in CC3 activity or lung uptake of DU. On the other hand, there was significant cellular infiltration in lungs of 60-hr hyperoxic rats as supported by the lung dry weight and histology. However, Howlett et al. reported that almost all TUNEL-positive cells in lungs of rats exposed to 100% O_2 for 60 hours were normal resident lung cells rather than inflammatory cells [18]. This suggests that apoptosis of invading inflammatory cells contributes little to the increased CC3 activity or enhanced DU lung uptake in the 60-hr hyperoxic lungs.

Exposure to 100% O_2 for 48 hrs had no effect on lung histology and was not associated with the development of pleural effusion, although the lung wet/dry weight increased by 15%. For 60-hr hyperoxic rats, the increase in lung wet weight was due to both increased tissue mass and edema as suggested by the increase in lung dry weight and wet/dry weight, respectively. Royston et al. measured the effect of rat exposure to 100% O_2 over 60 hrs on lung clearance of ^{125}I-bovine serum albumin as a measure of lung capillary endothelial

permeability [16]. They showed that permeability increased after 48 hrs and incremented sharply again after 60 hrs of exposure.

Hyperoxia-induced increases in lung tissue wet weight (Table 1) due to edema and/or cellular infiltration could increase the initial DU lung signal due to passive diffusion. However, that alone should not lead to an increase in DU lung steady-state uptake unless the edematous lung tissue volume has accessible PE and/or nonspecific DU binding sites. Otherwise, DU that diffused into the lung tissue due to increased endothelial permeability would diffuse back to the blood stream. Although nonspecific DU binding is possible, it is unlikely since DU has a high binding affinity and specificity to PE and relatively fast blood clearance [13,14]. In addition, changes in DU uptake in other organs or in cardiac output may contribute to changes in DU uptake in the *lung* with hyperoxia. Future studies using kinetic data (Figure 4) with a pharmacokinetic model will enable determination of the sensitivity of DU lung uptake to these potential changes.

Overall, lung DU uptake in vivo was increased after just 48 hours of >98% O_2 exposure, prior to the onset of any substantial histologic or functional evidence of lung injury. The large fraction of apoptotic lung cells that are endothelial cells and the strong correlation between the number of CC3 positive cells and DU lung uptake suggest that endothelial cells undergoing apoptosis contribute significantly to the enhanced DU lung uptake signal, and supports the utility of DU imaging for detecting hyperoxia-induced endothelial cell death in vivo. Since lung capillary endothelial cells are a primary and early target of injury associated with ALI, the results raise the potential utility of DU imaging for early detection of ALI or hyperoxic lung injury as a diagnostic measure. Early detection of injury could improve outcomes in ALI patients by better quantifying the extent of lung injury in an individual patient at a time when interventions are most effective.

ACKNOWLEDGEMENTS

This work was supported by NIH grants 8UL1TR000055 (CTSI) (Audi, Clough), 1R01HL116530 (Jacobs, Audi, Clough), and 5R01HL102085 (Zhao), VA Merit Review Award BX001681 (Jacobs, Audi, Clough), The Alvin and Marion Birnschein Foundation, and Marquette University Graduate School (Audi, Clough). Statistical analysis was supported by National Center for Advancing Translational Sciences, NIH grant 8UL1TR000055. The authors gratefully acknowledge the contributions of Dr. Naveen Bansal (Marquette University), Dr. Aniko Szabo and Ms. Natasha Sahr (Medical College of Wisconsin) in providing statistical consultation.

REFERENCES

1. Matthay MA, Zemans RL. The acute respiratory distress syndrome: pathogenesis and treatment. Annu Rev Pathol. 2011; 6:147–63. [PubMed: 20936936]
2. Gajic O, Dara SI, Mendez JL, Adesanya AO, Festic E, Caples SM, Rana R, St Sauver JL, Lymp JF, Afessa B, Hubmayr RD. Ventilator-associated lung injury in patients without acute lung injury at the onset of mechanical ventilation. Crit Care Med. 2004; 32:1817–24. [PubMed: 15343007]
3. Levitt JE, Matthay MA. Clinical review: Early treatment of acute lung injury - paradigm shift toward prevention and treatment prior to respiratory failure. Crit Care Med. 2012; 16:223.
4. Herasevich V, Yilmaz M, Khan H, Hubmayr RD, Gajic O. Validation of an electronic surveillance system for acute lung injury. Intensive Care Med. 2009; 35:1018–23. [PubMed: 19280175]
5. Kallet RH, Matthay MA. Hyperoxic acute lung injury. Respir Care. 2013; 58:123–41. [PubMed: 23271823]

6. Fisher AB, Beers MF. Hyperoxia and acute lung injury. Am J Physiol Lung Cell Mol Physiol. 2008; 295:L1066. author reply L1067. [PubMed: 19047485]
7. Crapo JD, Barry BE, Foscue HA, Shelburne J. Structural and biochemical changes in rat lungs occurring during exposures to lethal and adaptive doses of oxygen. Am Rev Respir Dis. 1980; 122:123–43. [PubMed: 7406333]
8. Rogers LK, Tipple TE, Nelin LD, Welty SE. Differential responses in the lungs of newborn mouse pups exposed to 85% or >95% oxygen. Pediatr Res. 2009; 65:33–8. [PubMed: 18703992]
9. Merker MP, Audi SH, Lindemer BJ, Krenz GS, Bongard RD. Role of mitochondrial electron transport complex I in coenzyme Q1 reduction by intact pulmonary arterial endothelial cells and the effect of hyperoxia. Am J Physiol Lung Cell Mol Physiol. 2007; 293:L809–19. [PubMed: 17601793]
10. Brueckl C, Kaestle S, Kerem A, Habazettl H, Krombach F, Kuppe H, Kuebler WM. Hyperoxia-induced reactive oxygen species formation in pulmonary capillary endothelial cells in situ. Am J Respir Cell Mol Biol. 2006; 34:453–63. [PubMed: 16357365]
11. Audi SH, Roerig DL, Haworth ST, Clough AV. Role of glutathione in lung retention of 99mTc-Hexamethylpropyleneamine oxime in two unique rat models of hyperoxic lung injury. J Appl Physiol. 2012; 113:658–65. [PubMed: 22628374]
12. Clough AV, Audi SH, Haworth ST, Roerig DL. Differential lung uptake of 99mTc-Hexamethylpropyleneamine oxime and 99mTc-Duramycin in the chronic hyperoxia rat model. J Nucl Med. 2012; 53:1984–1991. [PubMed: 23086010]
13. Audi S, Li Z, Capacete J, Liu Y, Fang W, Shu LG, Zhao M. Understanding the in vivo uptake kinetics of a phosphatidylethanolamine-binding agent (99m)Tc-Duramycin. Nucl Med Biol. 2012; 39:821–5. [PubMed: 22534031]
14. Zhao M, Li Z, Bugenhagen S. 99mTc-labeled duramycin as a novel phosphatidylethanolamine-binding molecular probe. J Nucl Med. 2008; 49:1345–52. [PubMed: 18632826]
15. Ali I, Gruenloh S, Gao Y, Clough A, Falck JR, Medhora M, Jacobs ER. Protection by 20-5,14-HEDGE against surgically induced ischemia reperfusion lung injury in rats. Ann Thorac Surg. 2012; 93:282–8. [PubMed: 22115333]
16. Royston BD, Webster NR, Nunn JF. Time course of changes in lung permeability and edema in the rat exposed to 100% oxygen. J Appl Physiol. 1990; 69:1532–7. [PubMed: 2262477]
17. Kawamura T, Wakabayashi N, Shigemura N, Huang CS, Masutani K, Tanaka Y, Noda K, Peng X, Takahashi T, Billiar TR, Okumura M, Toyoda Y, Kensler TW, Nakao A. Hydrogen gas reduces hyperoxic lung injury via the Nrf2 pathway in vivo. Am J Physiol Lung Cell Mol Physiol. 2013; 304:L646–56. [PubMed: 23475767]
18. Howlett CE, Hutchison JS, Veinot JP, Chiu A, Merchant P, Fliss H. Inhaled nitric oxide protects against hyperoxia-induced apoptosis in rat lungs. Am J Physiol. 1999; 277:L596–605. [PubMed: 10484468]
19. Otterbein LE, Chin BY, Mantell LL, Stansberry L, Horowitz S, Choi AM. Pulmonary apoptosis in aged and oxygen-tolerant rats exposed to hyperoxia. Am J Physiol. 1998; 275:L14–20. [PubMed: 9688930]
20. Sun Q, Cai J, Liu S, Liu Y, Xu W, Tao H, Sun X. Hydrogen-rich saline provides protection against hyperoxic lung injury. J Surg Res. 2011; 165:e43–9. [PubMed: 21067781]
21. Von Jagow G, Bohrer C. Inhibition of electron transfer from ferrocytochrome b to ubiquinone, cytochrome c1 and duroquinone by antimycin. Biochim Biophys Acta. 1975; 387:409–24. [PubMed: 166667]

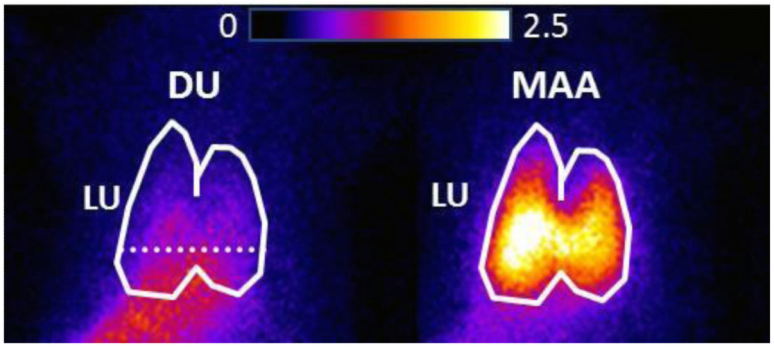

Fig. 1.

Planar images of a normoxic rat imaged 19 min following a first injection of ^{99m}Tc-duramycin, DU, (left) and then five minutes later with a subsequent injection of ^{99m}Tc-MAA (right). Lung (LU) ROI is identified in the MAA image, with the dashed horizontal lower boundary to avoid liver contribution. The ^{99m}Tc-MAA generated lung ROI mask was then superimposed on the DU image yielding the lung DU ROI.

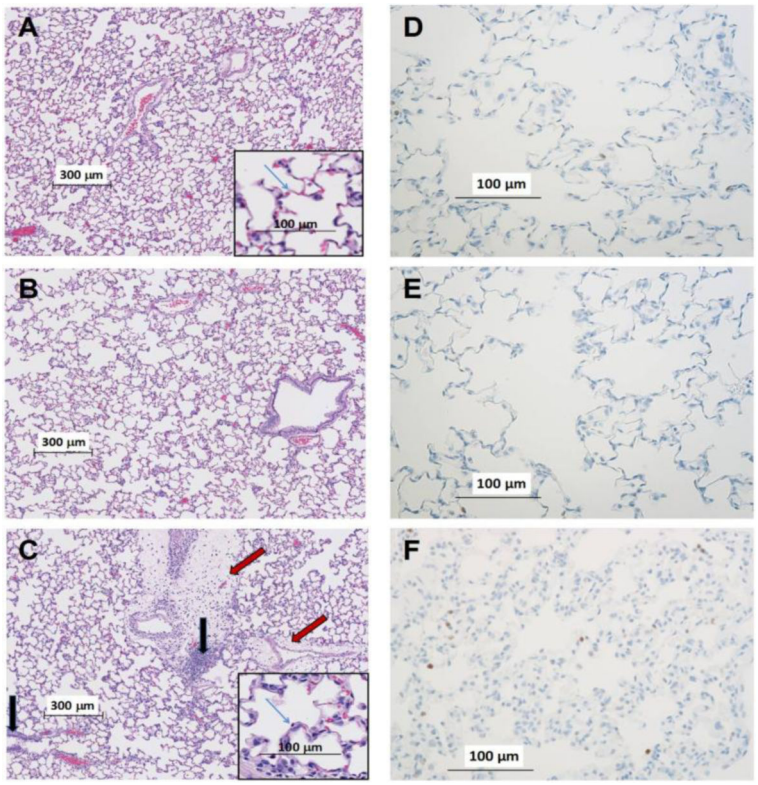

Fig. 2.

Representative images of normoxic (A), 48-hr hyperoxic (B), and 60-hr hyperoxic (C) H&E stained lung slices. Insets at higher power illustrate structural features. Red arrows point to perivasuclar edema in 60-hr slice. Blue arrows identify the alveolar capillary membrane. Black arrows point to inflammatory cells within the perivascular spaces. Representative images of normoxic (D), 48-hr hyperoxic (E) and 60-hr hyperoxic (F) lungs where myeloperoxidase positive cells appear brown

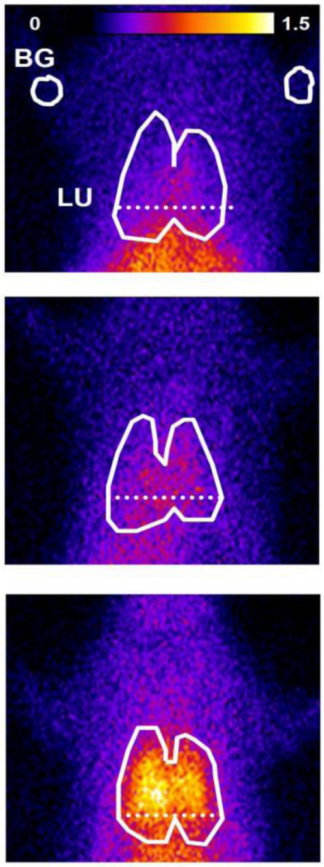

Fig. 3.

Planar images of ^{99m}Tc-duramycin, DU, distribution in a normoxic (top), 48-hr hyperoxic (middle) and 60-hr hyperoxic (bottom) rat 19 min following DU injection. Lung (LU) ROI is determined from the MAA image with the dashed horizontal lower boundary to avoid liver contribution, and background (BG) ROIs from upper forelimbs

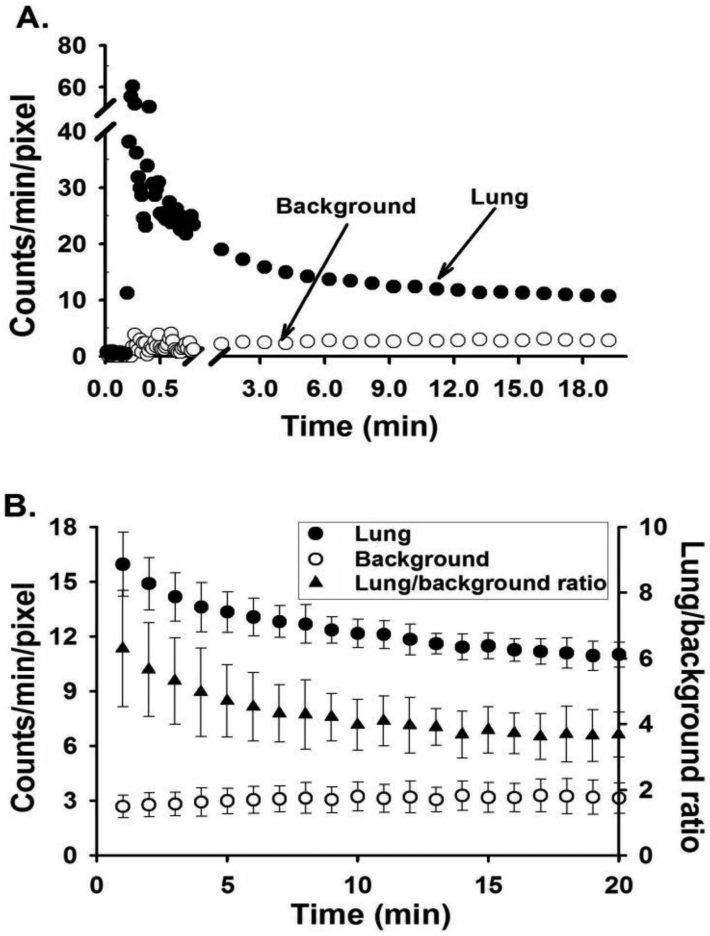

Fig. 4.

A. Representative normoxic ^{99m}Tc-duramycin, DU, time-activity curves acquired from lung and background ROIs. ***B.*** Average (mean ± SD) DU time-activity curves acquired from lung and background ROIs, and corresponding lung uptake (lung-to-background ratio) of the ten normoxic rats imaged

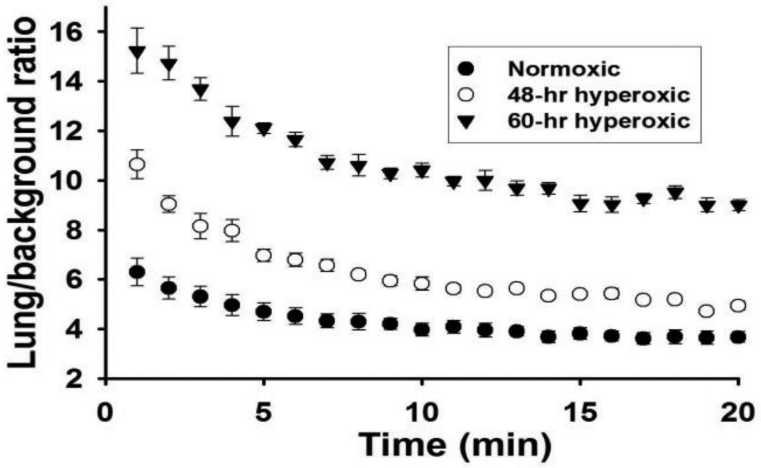

Fig. 5.

Lung uptake (lung-to-background ratio) of ^{99m}Tc-duramycin in normoxic (n = 10), 48-hr hyperoxic (n = 7), and 60-hr hyperoxic (n = 7) rats imaged. Values are mean ± SEM

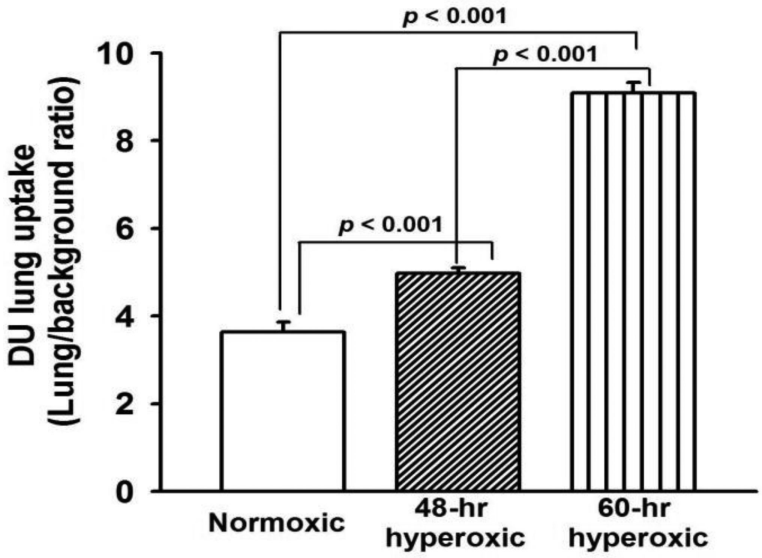

Fig. 6.

^{99m}Tc-duramycin, DU, lung uptake of normoxic (n =10), 48-hr hyperoxic (n =7), and 60-hr hyperoxic (n = 7) rats. Values are mean ± SEM. One-way ANOVA followed by Tukey's range test ($p < 0.05$) was used to evaluate differences among means of the three groups

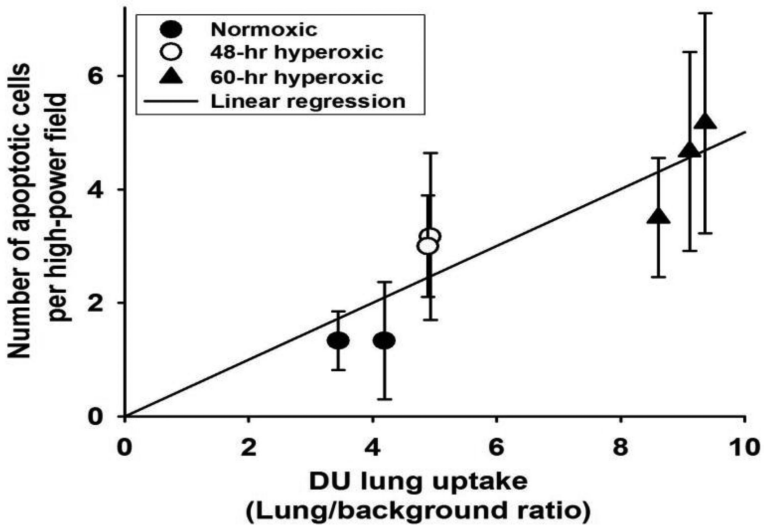

Fig. 7.

Correlation between ^{99m}Tc-duramycin, DU, lung uptake and corresponding number of cleaved caspase 3 (CC3) positive cells per high-power field in lung slices (6 slices per lung) for each of 7 rats (two normoxic, two 48-hr hyperoxic, and three 60-hr hyperoxic). Values of CC3 positive cells are mean ± SD. Coefficient of determination = 0.82 (Pearson Product Moment Correlation test, $p = 0.005$)

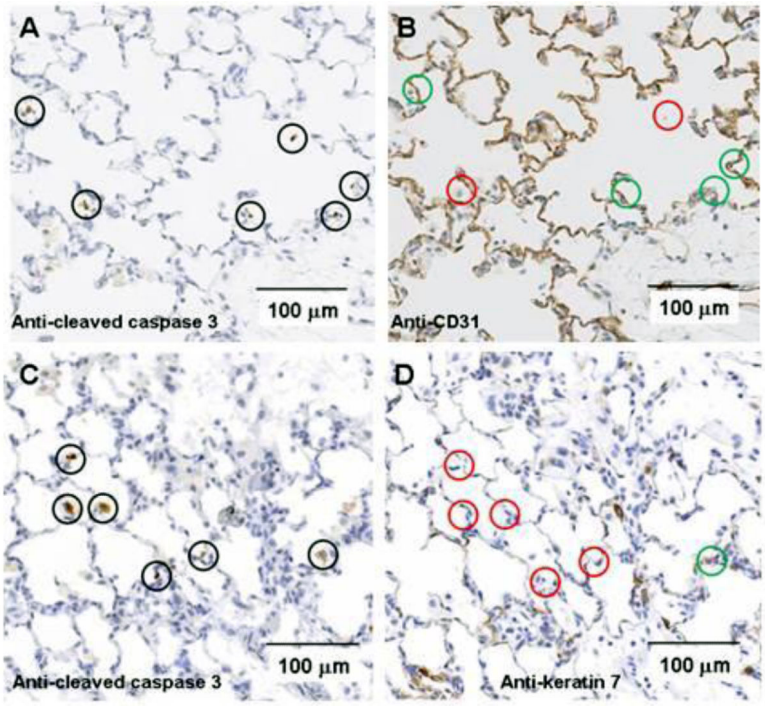

Fig. 8.

Panels A, B: Images of lung from a 60 hr hyperoxic rat stained with cleaved caspase 3 were selected blindly. Positive cells identified by brown stain are denoted by black circles. Consecutive slices were stained with a primary antibody for CD31 for endothelial cells. Analogous cells positive for cleaved caspase 3 were identified on CD31 slices, and marked as CD 31 positive (green circles) or negative (red circles). Of 85 cleaved caspase 3 positive cells, 45 (53%) were positive for CD 31. *Panels C, D:* Analogous to panels A&B except sequential slices were stained with a primary antibody for keratin 7 for epithelial cells. Of 59 CC3 positive cells, 10 (17%) were keratin 7 positive (green circle) and the remainder negative (red circles).

TABLE 1

Lung weights and pleural effusion weight

	Wet weight (g)	Dry weight (g)	Wet/dry ratio	Pleural effusion weight (g)
Normoxic	1.21 ± 0.04 n = 6	0.232 ± 0.007 n = 6	5.23 ± 0.10 n = 6	0 n = 6
48-hr hyperoxic	1.44 ± 0.09 n = 5	0.237 ± 0.008 n = 5	6.04 ± 0.02 * n = 5 (p = 0.018)	0 n = 5
60-hr hyperoxic	2.01 ± 0.09 *, & n = 5 (p <0.001)	0.321 ± 0.017 *, & n = 5 (p < 0.001)	6.28 ± 0.23 * n = 5 (p = 0.003)	7.6 ± 1.6 *, & n = 6 (p < 0.001)

Values are mean ± SEM. n is the number of rats. One-way ANOVA followed by Tukey's range test (p < 0.05) was used to evaluate differences among means of the three groups:

* significantly different from normoxics,

& significantly different from 48-hr hyperoxics.

TABLE 2

Results of immunohistochemistry studies

	Normoxic	48-hr hyperoxic	60-hr hyperoxic
Apoptotic cells per high-power field	1.3 ± 0.2 * n = 4	3.2 ± 0.1 * n = 6	4.7 ± 0.3 * n = 5 (p = 0.002)
% of CC3 positive cells that are CD31 positive	27 ± 6 * n = 4	59 ± 4 * n = 4 (p = 0.002)	53 ± 4 * n = 4 (p = 0.007)
% of CC3 positive cells that are keratin 7 positive	44 ± 8 * n = 4	22 ± 4 * n = 4	17 ± 4 * n = 4 (p = 0.019)
% of CC3 positive cells that are unknown	30 ± 8 n = 4	19 ± 6 n = 4	29 ± 7 n = 4
Average MPO thresholded area × 10^{-2}	37.5 ± 4.8 * n = 5	35.5 ± 4.2 * n = 4	68.0 ± 10.1 *, & n = 4 (p = 0.02)

Values are mean ± SEM. n is the number of rats. Kruskal-Wallis one-way ANOVA on ranks followed by Dunn's method ($p < 0.05$) was used for statistical analysis of the differences in the number of apoptotic cells per high-power field among means of three groups. Otherwise, oneway ANOVA followed by Tukey's range test ($p < 0.05$) was used to evaluate differences among means of the three groups.

* significantly different from normoxics,

& significantly different from 48-hr hyperoxics.